A Novel Integration of Stereolithography and Inkjet Printing for Multichip Modules with High Frequency Packaging Applications

Ryan Bahr, Bijan Tehrani, Manos M. Tentzeris
Electrical and Computer Engineering
Georgia Institute of Technology
Atlanta, United States of America
rbahr3@gatech.edu, btehrani3@gatech.edu

Kyle Byers
DOE's Kansas City National Security Campus
Managed by Honeywell FM&T
Kansas City, United States of America
kbyers@kcp.com

***Abstract*—Within this paper methods of additive manufacturing for 3D circuitry is discussed. With increasing interest in the additive manufacturing of 3D circuits, varying topologies must be explored and tested to create frameworks for how to fabricate topologies with the wide design space that is introduced with additive manufacturing and 3D printing. After discussing current methods of additive manufacturing of electronics and the current limitations of different methodologies, several topologies are discussed for the inclusion of surface mount technology components with 3D printing using inkjet printing and stereolithography, including the use of inkjet printed adhesives for placement of components. Finally, a planar inverted-F antenna is integrated into the substrate, to create a complete system for a ZigBee multi-chip module utilizing additive manufacturing techniques.**

Keywords-3D printing, additive manufacturing, stereolithography, inkjet printing, multichip module (MCM), planar inverted-F antenna (PIFA), surface mount technology, Zigbee, SU-8.

I. INTRODUCTION

In the last 10 years, additive manufacturing has seen exponential growth with the constant development of new fabrication utilities, and novel applications from the increased versatility of the tools available. While some 3D technologies existed since the late 1970's only recent advancements have been made towards achieving 3D printed or otherwise additively manufactured electronics. Methods such as inkjet printing have enabled multilayered high resolution designs which, most importantly, can be scaled for large surface areas. Stereolithography (SLA) 3D printing is primarily limited by optics, enabling high resolution designs. With the digital light projection (DLP) SLA printing, many designs can be printed simultaneously with photopolymer resins without any additional fabrication time, enabling scalability of both small and large designs. More importantly with SLA technologies, low surfaces roughness of 400 nm peak-to-peak have been measured, providing surfaces to inkjet print silver nanoparticle (SNP) inks without introducing discontinuities due to surface roughness, maintaining a conductivity of 5e6 s/m [1].

These technologies combined enable the printing of RF microelectronics for millimeter wave (mm-Wave) applications with reduction in losses due to surface roughness. The combination of both inkjet printing and 3D printing enables a dynamic range of resolutions, with z-layer heights from 500 nm to exceeding 100 μm, and XY minimum feature sizes from 20-40 μm, as well as a wide range of materials so long as they conform to the viscosity and particle size requirements of inkjet or the photo-curability requirements necessary in SLA printing [2].

Inkjet printing has been successfully combined with 3D SLA printing for packaging interconnects up to 70 GHz [1]. In this paper, it is demonstrated how to integrate passive devices such as surface mount technology (SMT) components and antennas. Characterization of features such as cavities and adhesives is discussed in terms of the minimum resolution available, feasible design space, and materials available for this novel approach to multimaterial 3D printing for high frequency electronics. The designs can be directly be printed onto a wide range of substrates, enabling the addition of smart devices into existing systems.

The use of these topologies combined are utilized to create a full system with SMT components and integrated planar inverted-F antenna (PIFA) for a fully printed 2.4 GHz ZigBee multichip module (MCM) for internet of things (IoT) applications utilizing a CC2520 ZigBee module and CC2590 2.4 GHz range extender.

II. ADDITIVE MANUFACTURING OF 3D ELECTRONICS

A wide variety of 3D printing methods exists, with the original intent to create reproductions of models to evaluate dimensions and practicality of designs. For quite some time, there have been great efforts to functionalize the field, which became to be known as additive manufacturing (AM). With high strength metal deposition, developments have enabled low part count, high complexity rocket nozzles with reduced weight critical for space applications. 3D prints incorporating metamaterials enable single part, single material reconfigurable functionality [2]. Only within the last several years has there been development in printing processes that process both conductors/metals and polymers simultaneously. Selective metallization is generally the most challenging factor, often limited by either material properties, deposition tools, or a combination thereof.

A common method of multimaterial deposition was the use of direct write systems. Recent interest in this becoming commercially viable have been demonstrated with depositions such as the Voxel8, based on previously published silver inks, utilizing fused deposition modeling (FDM) printing combined with a syringe deposition direct write system [3]. The Hyrel 3D line of FDM printer systems enables multiple customizable methods, enabling hybrid FDM and direct write

2377-5726/18/$31.00 ©2018 IEEE
DOI 10.1109/ECTC.2018.00376

methods [4]. Many laboratories will develop their own direct write methodologies due to the ever-increasing demands of resolutions, materials, and unique mechanics that are required for specific projects. Higher resolution direct-write techniques utilizing specialized pumps have achieved resolutions of 14 μm, utilizing an nScrypt printer and pump, which enables interesting packaging applications such as the ability to print high viscosity pastes for applications such as 3D printed LTCC packaging [5].

More recent advancements have been made to advance scalability of high resolution multimaterial deposition. 3D printing with inkjet systems enables high resolution, typically down to 20 μm, and an extremely wide gamut of materials while being moderately scalable due to multi-head systems with 1024 nozzles per head already utilized in industry [6]. Most notable is Nano Dimensions Dragonfly line of printers, which enable the deposition of nanoparticle inks and dielectrics simultaneously which are sintered with a laser. Some of the most recent research has demonstrated multi-material inkjet printing where the use of a Meyer Burger PiXDRO LP50 with multiple print heads has demonstrated 3D metallic structures and multimaterial structures as seen in [7].

LPKF also has a notable method of selective metallization of 3D models using Laser Direct Structuring (LDS). Taking either 3D printed or molded parts, a proprietary spray is deposited on the entire surface of a model [8]. Utilizing a multi axis laser sintering system to activate the spray to the surface of the part utilizing an IR laser with a focused diameter of 50 ±5 μm, followed by submerging the entire part into an electroless depositing solution.

There are additional methods of metallic deposition that of interest. Aerosol jet printing is currently one of the highest resolution printing methods, often reaching resolutions as low as 10 μm, and similar to inkjet printing, is a non-contact method. The viscosity requirements are not as strict as inkjet printing, enabling a wider range of materials, and often performed on a multi-axis system due to the propellent gas enabling performance that is more consistent.

III. Methods of Intergration of Discrete Componenets

The ultimate accomplishment for additive manufacturing of electronics is to provide design specs that may approach or exceed modern circuit board design while offering additional features, such as integration of 3D antennas, hermetic seals, dielectric lenses, and 3D interconnects that minimize losses and electromagnetic interference (EMI). Integration with bare die and off-the-shelf available components will be a necessity for additive manufacturing to compete long term with present technologies.

The integration of modern electronics with additive manufacturing methodologies will need continuous development and characterization as each year new printers, materials, and processes are developed, offering unique and process-specific topologies.

Direct deposition processes (aerosol jet, inkjet, direct write, etc) tend to have physical limitations in the deposition process that often limits the resolution of the minimum feature size to that of 5-20 μm, depending on the process and materials. For example, inkjet printing resolution is often limited by the inkjet head nozzle volume with 1 pl often one of the lowest commercially available sizes. Due to the radius vs volume of a sphere, to increase the resolution by decreasing the radius size the volume must be reduced by the cubic root, which imposes challenges to achieve sub-micron resolutions [9].

Other topological layouts, such as embedding SMT components within a print may be challenging in a multilayer fashion with the LDS methodology, though simultaneously the technology may excel at placing components on multiple non-parallel planes. Nano-Dimension's DragonFly 2020 printers have recently demonstrated embedded SMD components, which offers protection from external elements such as mechanical, temperature or corrosion factors [10].

Methods to achieve submicron resolution additive manufacturing will have to rely on optic-based tools. Laser based processes can create submicron features, with 2-photon polymerization enabling features as low as 100 nm. Unfortunately, selective metallization with said technology is not possible yet. Variations of LDS or Nano-Dimension's use of a laser sintering may be used in the future to further increase resolutions.

The utilization of stereolithography and inkjet printing technologies enables a combination of rapid prototyping to produce optically limited, low surface roughness dielectrics and deposition limited conductors, paving the way for mm-Wave electronics. This enables thick film dielectrics more than 100 μm thick, while allowing and thin film conductors below 500 nm [11]. Utilizing a modified LittleRP open source digital light projection (DLP) stereolithography (SLA) printer, we can enable multimaterial printing for multiple dielectrics, including those loaded with ceramic particles and embedded inkjet printing for conductors [1]. DLP SLA enables the printing of multiple structures simultaneously, in a similar process to maskless lithography in typical semiconductor fabrication, where resolutions have exceeded 1 μm.

IV. Consideration of Surface Rougness

Many printing technologies have not been fully characterized due to their innovative processes that are just beginning to be adopted for electronic purposes, as well as the wide variation in printing recipes which cause wide variations of properties. Previous combining stereolithography and inkjet printing has demonstrated the feasibility of selective metallization additive manufacturing for interconnects up to 90 GHz reaching the end of the E band. While low resistivity materials have been a figure of merit for many conductive printing technologies, low surface roughness is equally important to reduce conductor losses for high frequency applications. As the losses approach the thickness of the skin depth, surface roughness increases conductor losses by approximately 60% and approach a 100% increase in losses as the roughness becomes much larger than the surface roughness [12]. In (1), the equivalent surface resistance R_s is related to the R_Q is the root-mean-square (RMS) roughness, the operational frequency f, the electrical resistivity ρ, and the magnetic permeability μ.

$$R_s = \left(1 + \frac{2}{\pi}\tan^{-1}\left(1.4 \times {R_Q}^2 \times \frac{\pi\mu f}{\rho}\right)\right) \quad (1)$$

Utilizing a modified LittleRP open source DLP stereolithography (SLA) printer with Vorex Orange acrylate resin, a surface roughness of 98 nm R_Q and approximately 400 nm peak-to-peak was measured with a profilometer. Silver nanoparticle ink with 5 layers deposited and sintered at 200 °C maintain a conductivity of 1.2 x 10^7 S/m, correlating to a frequency of operation beyond terahertz before surface roughness effects increase conductor losses by 60%, which can further be improved with passivation with inkjet-printed dielectrics [13]. The surface roughness is orders of magnitude lower than FDM methods [14], where even 1 µm of surface roughness would cause 60% in conductive losses at 21 GHz at an identical conductivity. and confirms the ability for inkjet and SLA to perform for high frequency applications for mm-Wave and next generation applications.

V. Proposed Topologies of Interconnects

Due to the wide variety of topologies available to both stereolithography and inkjet printing, a few methods of component integration were demonstrated that utilized strengths of either technology, and there exist plenty due to the wide design space of 3D printing. Within this paper, methods that integrate SMT components directly into the SLA substrate are prototyped. Thereafter, a novel use of SU-8 to attach SMT components is tested for feasibility to improve shear strength on the surface of substrates. Finally, the prototype is printed utilizing inkjet printing and direct-write pastes.

A. Stereolithography Integrated SMD Componenets

The integration of electronics and stereolithography has only been recently accomplished, often using top-down stereolithography machines, where the build platform submerges lower into a vat of photopolymer as the 3D print progresses [15]. In this approach a flat surface is printed, the SMT components are attached to the substrate, and printing continues. Bottom-Up stereolithography has several advantages including significantly less material waste, integration of multiple photopolymer resins, reduced oxygen inhibition of polymerization, and reduced surface roughness, but poses a challenge to integrate discrete components. The reasoning for this is the build plate is pressed flush against a transparent surface to build layers up, and attached discrete components that are larger than the printing layer thickness will be compressed against the transparent window, likely causing damage to the component or the window, as seen in Figure 1.

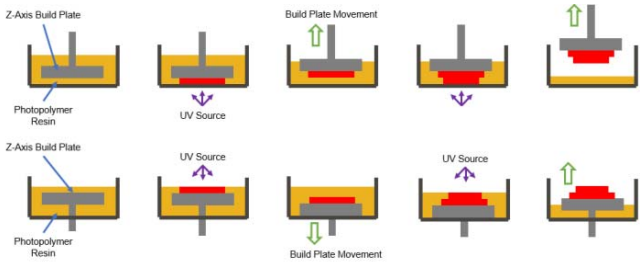

Figure 1. Bottom-up stereolithography printing processes (top) as used in this paper and top-down (bottom) stereolithography [16].

Two solutions are apparent to attempt to integrate discrete components. The first would be to increase the layer thickness for that specific layer to prevent the component from touching the transparent window. This sacrifices resolutions but also comes with a dependency of the thickness of the component, and utilizing multiple components of different thicknesses may cause the thinnest component to be in a cavity. The components would optimally be metalized at the bottom of the component if it were desired for them to be connected on the same plane. The alternative solution is to print cavities (of different depths depending on components) and place the components in said cavities, which would cause the tops of the cavities/SMT devices to all be on the same plane and could then interconnect from there, essentially becoming an upside-down PCB, which opens up a new set of design rules. This would also expose the underside of integrated circuit (IC) if integrated with the system, enabling easier interconnections to IC packages that only have leads on the bottom. This is especially beneficial with the use of silver pastes and direct write methodologies.

Several considerations must be made regarding this methodology. First, printing orientation can have significant effects due to cure-through, as seen in Figure 2. This may be improved with custom photopolymer recipes that increase the %w of UV blocker to prevent curing too much during overhangs and bridges in 3D models. Additionally, air may get trapped after placement of SMT components and steps should be taken to remove air. The utilization of inkjet printing with this topology may prove difficult as the slightest formation of a crevice will cause capillary action with low viscosity conductive inks, possibly causing a short as the liquid is distributed across the entire crevice around the SMT component. The use of a low viscosity dielectric ink to fill any crevices that occur before the printing of conductors may be beneficial to prevent capillary effects of the silver nanoparticles inks.

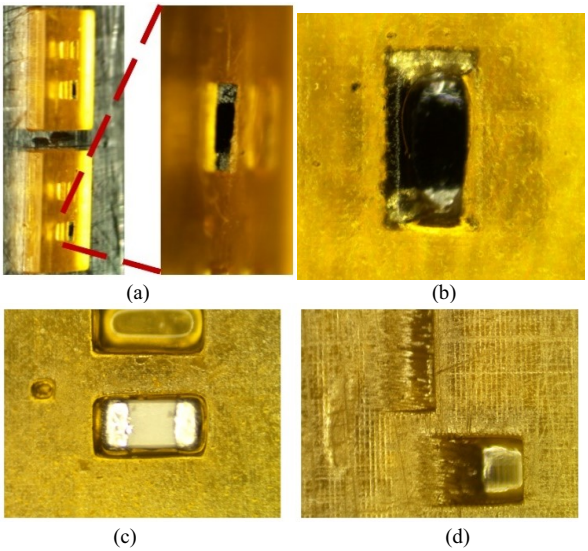

Figure 2. SMT resistor placed in cavity (a) and then encapsulated (b). Print orientation depedency of stereolithography. (c) Substrate printed parallel and (d) perpendicular to build plate.

B. InkJet Printed SU-8 for SMT Attach

An advantage of printing the crevices and placing components in the crevices is that the components are held in place for metallization. Previous research has demonstrated that the metallization of SMT devices with inkjet printing can be utilized for mounting of devices [17—19]. Unfortunately, after attempting to print device solely with SNP inks, the SMT components of 0402 sizing detached often with normal handling.

In order to take advantage of the multi-material inkjet printing, SU-8 photoresist is used in conjunction with SNP inks to for SMT adhesive purposes similar to those used in wave soldering applications. In wave soldering applications, specific adhesives are deposited using direct write methods, often utilizing one or two dots of material with syringe deposition which leads [20]. SU-8 has demonstrated significant properties for packaging applications in both additive manufacturing technologies and traditional semiconductor manufacturing [21, 22]. With inkjet printing, the pattern of the adhesive can be tailored to create specific patterns, such as a square to maximize the surface area, as shown in Figure 3, and increase the total force necessary to shear devices. Five layers of SNP ink are printed and sintered at 200 °C for 1 hour, and two layers are of SU-8 are printed for adhesion purposes with a 500.0 mJ/cm^2 exposure to crosslink the photoresist.

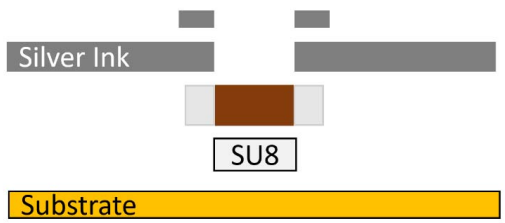

Figure 3. Proposed topology of SMD adhesion.

A Condor Sigma bond tester with shear capability is utilized to determine the sheer capabilities of resistors with printed adhesives. The SU-8 covers a surface of 0.7 mm × 0.5 mm between the SMT and substrate, and the silver overlaps 0.1 mm × 0.5 mm on both pads of the resistors. In Figure 4 the SU-8 adhesive is visible underneath the resistors. A 50 µm thick Kapton polyimide substrate is utilized for more results that are easier to compare to previous studies. The peak force before shearing was 1.19 kgf, which results in a shear force of 23.3 MPa which demonstrates performance that significantly exceeds that of only silver nanoparticles by over an order of magnitude [17]. The traces are 500 µm wide and 4.6 mm long per each lead for a total length of 10 mm after inclusion of 0402 resistor. The probes of a DMM measured 0.218 Ω, and directly connected to an 0402 had a 0.245 Ω resistance, leading to a 0.027 Ω contact resistance between probes and SMT devices. Total resistance of these traces were measured to be 0.317 ± 0.011 Ω and demonstrates significantly lower contact resistance compared to previous work [17].

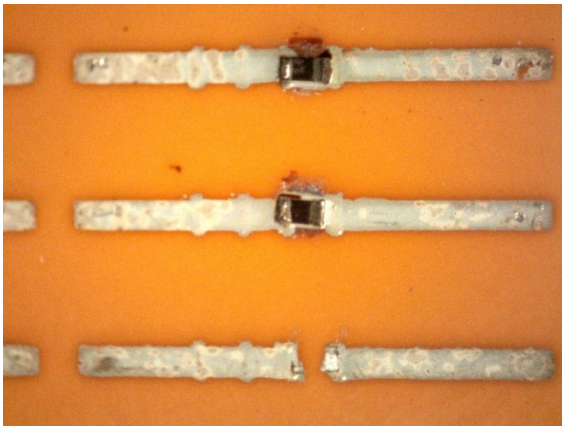

Figure 4. InkJet printed adhesive SU-8 pads and SNP ink interconnects on 80 µm Kapton polymide. The top two rows have visible SU-8 beneath the resistors, where the last row the 0402 resistor flew off with regular handling.

C. PIFA Antenna Design

The use of additive manufacturing techniques for printing substrates enables the ability to fabricate complex structures, including gradient index (GRIN) materials, variable thicknesses, and variable dielectric constants which can be used to modify the substrate properties at a system designers' discretion and enable additional design space for improved radiation, matching, and coupling properties [2]. Photopolymers tend to be lossy, and there is current research into improving the electrical properties of 3D printed substrates for electromagnetic purposes [23, 24].

PIFA antennas offer exceptional omnidirectional performance in compact form factors, and are currently implemented in many consumer products, often with several of them in a single active device. On a two millimeter thick substrate of Vorex Orange (ε_r =2.65, tanδ = .017), a 50 Ω PIFA antenna is designed for 2.45 GHz. The PIFA was designed based upon the quarter electrical wavelength of 18.8 mm, and

a Trust Region Framework optimization algorithm within CST MICROWAVE STUDIO®, with the final model demonstrated in Figure 5. The length of the PIFA is 23.02 mm with the feed and short posts separated by 3.04 mm, and the antenna is 4.55 mm offset from the ground plane. Widths of all lines are 1.05 mm. The maximum realized gain is 1.714 dB. In Figure 6 the model that is manufactured with the appropriate interconnects for measuring the radiation pattern is demonstrated. The return loss in measured and presented in Figure 7, with a secondary resonance apparent. The resonance may possibly be caused due to issues related to the silver epoxy that is used to connect the through substrate via for the shortening pin. The antenna was simulated with both an SMA connector and without one to verify that it has little effect on the omnidirectional pattern of the antenna. In Figure 8, the normalized radiation pattern is verified showing agreement between simulated model and fabricated model.

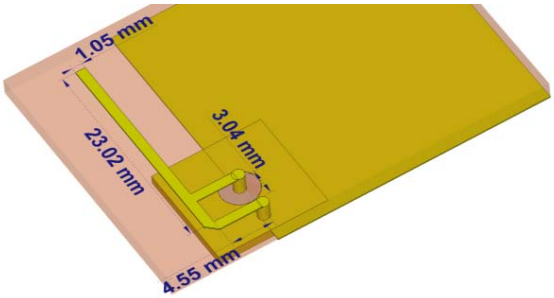

Figure 5. Antenna simulation model with panel mount SMA connector, excited with a waveguide port.

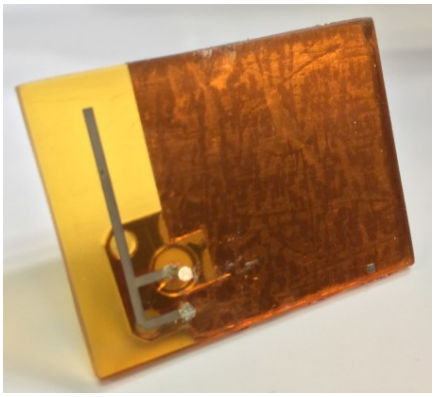

Figure 6. Fabricated model of PIFA.

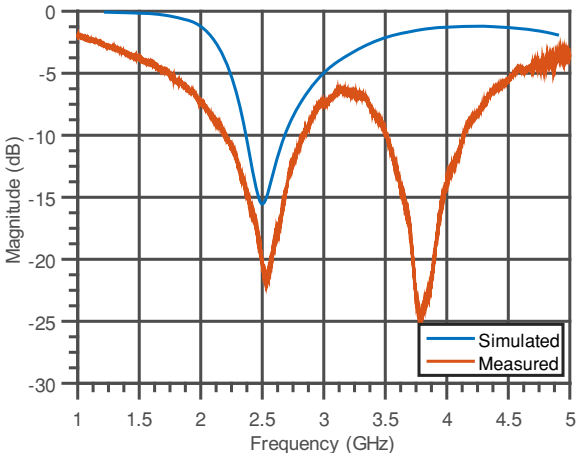

Figure 7. PIFA simulated vs measured resturn loss.

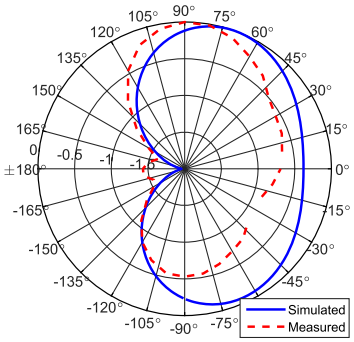

Figure 8. PIFA radiation pattern simulated vs measured at 2.44 GHz, along the azimuth plane.

D. Additively Manufactured MCM

Utilizing the techniques discussed, a complete system is additively manufactured using a combination of said techniques. A substrate made with stereolithography is fabricated on a LittleRP printer. Two ZigBee-based chips were selected from Texas Instruments to enable IoT functionality with 3D printed packaging for future applications. The CC2520 ZigBee module containing an IEEE 802.15.4/Zigbee compatible transceiver and a CC2590 2.4 GHz range extender, containing an internal power amplifier (PA), low noise amplifier (LNA), switches, RF matching, and balun. Circuitry consists of inkjet printing for the interconnects, ground planes, and antennas. Silver epoxy is utilized for many of the SMT resistors, capacitors, and inductors. All SMT RLC components are 0402. The CC2520 is a QFN-28 had pads of .28 mm width and .5 mm pitch. The CC2590 is a QFN-16 with pads of .35mm width and a .65 mm pitch. Components are placed utilizing a manual pick and place machine. The silver ink is cured first at 200 °C and the

silver epoxy on a second bake at 100 °C. The fully fabricated prototype is presented in Figure 9.

Future work will involve the programming and utilization of the MCM for IoT applications and evaluating real world performance for mesh networking applications.

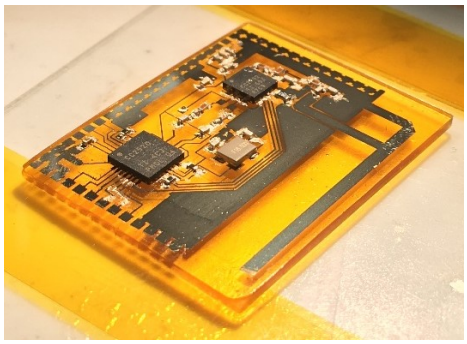

Figure 9. Inkjet printed MCM device on SLA printed substrate

VI. Conclusion

A variety of topologies have been investigated for the use of stereolithography 3D printing of MCM systems. The capabilities of multimaterial printing for electronic device prototypes enables the integration of additional components, including interconnects, on-board antennas, and cavity structures. The use of adhesives enables placement of components similar to that of traditional manufacturing with PCB adhesives, and shows significant improvements compared to previously demonstrated results for conductivity and shear strength. Based on the acquired knowledge, a full 2.4 GHz Zigbee system is fabricated utilizing both inkjet and stereolithography, demonstrating the future use of additive manufacturing and IoT devices.

Acknowledgments

The authors would like to acknowledge Honeywell for supporting this work.

References

[1] B. Tehrani, R. Bahr, W. Su, B. Cook, and M. Tentzeris, “E-Band Characterization of 3D-Printed Dielectrics for Fully-Printed 3D Wireless System-on-Package Integration,” 2017 IEEE MTT-S International Microwave Symposium (IMS), Honolulu, Hawaii, USA, Jun 2017.

[2] J. G. Hester et al., "Additively Manufactured Nanotechnology and Origami-Enabled Flexible Microwave Electronics," in Proceedings of the IEEE, vol. 103, no. 4, pp. 583-606, April 2015.I. S. Jacobs and C. P. Bean, “Fine particles, thin films and exchange anisotropy,” in Magnetism, vol. III, G. T. Rado and H. Suhl, Eds. New York: Academic, 1963, pp. 271–350.

[3] J. Smay, J. Cesarano and J. Lewis, "Colloidal Inks for Directed Assembly of 3-D Periodic Structures", *Langmuir*, vol. 18, no. 14, pp. 5429-5437, 2002.

[4] T. Le *et al*., "A novel strain sensor based on 3D printing technology and 3D antenna design," *2015 IEEE 65th Electronic Components and Technology Conference (ECTC)*, San Diego, CA, 2015, pp. 981-986.

[5] Xudong Chen, Kenneth Church, Ali Karbasi, and W. Kinzy Jones (2013) Micro-Dispense Direct Printing for Thermal Management Structure Using LTCC. Additional Conferences (Device Packaging, HiTEC, HiTEN, & CICMT): September 2013, Vol. 2013, No. CICMT, pp. 000221-000225.

[6] D. Stüwe, D. Mager, D. Biro and J. Korvink, "Inkjet Technology for Crystalline Silicon Photovoltaics", *Advanced Materials*, vol. 27, no. 4, pp. 599-626, 2014.

[7] E. Saleh, F. Zhang, Y. He, J. Vaithilingam, J. Fernandez, R. Wildman, I. Ashcroft, R. Hague, P. Dickens and C. Tuck, "3D Inkjet Printing of Electronics Using UV Conversion", *Advanced Materials Technologies*, vol. 2, no. 10, p. 1700134, 2017.

[8] LPKF, "LPKF-LDS Process (Laser Direct Structuring) LPKF Laser & Electronics AG", *LPKF.com*, 2018. [Online]. Available: http://www.lpkf.com/applications/mid/lpkf-lds-process/. [Accessed: 23- February- 2018].

[9] S. Jung, "Fluid characterisation and drop impact in inkjet printing for organic semiconductor devices", Ph. D, University of Cambridge, 2011.

[10] N. Dimension, "Dragonfly 2020 Pro", *Nano-di.com*, 2018. [Online]. Available: http://www.nano-di.com/dragonfly-2020-pro. [Accessed: 23- February- 2018].

[11] E. O. Hammerstad and F. Bekkadal, “A microstrip handbook,” ELAB Report, STF44 A74169, Univ. of Trondheim, Norway, 1975, pp. 98–110.

[12] Tehrani, B., Mariotti, C., Cook, B., Roselli, L. and Tentzeris, M. (2016). Development, characterization, and processing of thin and thick inkjet-printed dielectric films. *Organic Electronics*, 29, pp.135-141.

[13] B. S. Cook and A. Shamim, ‘‘Inkjet printing of novel wideband and high gain antennas on low-cost paper substrate,’’ *IEEE Trans. Antennas Propag*., vol. 60, no. 9, pp. 4148–4156, Sep. 2012.

[14] D. K. Ahn, S. M. Kwon and S. H. Lee, "Expression for Surface Roughness Distribution of FDM Processed Parts," *2008 International Conference on Smart Manufacturing Application*, Gyeonggi-do, 2008, pp. 490-493.

[15] Joe Lopes, Amit, Eric MacDonald, and Ryan B. Wicker. "Integrating Stereolithography and Direct Print Technologies For 3D Structural Electronics Fabrication". *Rapid Prototyping Journal* 18.2 (2012): 129-143. Web. 15 Feb. 2017.

[16] Tehrani, B., Bahr, R. and Tentzeris, M. (2017). Inkjet and 3D Printing Technology for Fundamental Millimeter-Wave Wireless Packaging. *International Symposium on Microelectronics*, 2017(1), pp.000252-000257.

[17] J. Arrese, G. Vescio, E. Xuriguera, B. Medina-Rodriguez, A. Cornet and A. Cirera, "Flexible hybrid circuit fully inkjet-printed: Surface mount devices assembled by silver nanoparticles-based inkjet ink", *Journal of Applied Physics*, vol. 121, no. 10, p. 104904, 2017.

[18] H. Andersson, A. Manuilskiy, S. Haller, M. Hummelgård, J. Sidén, C. Hummelgård, H. Olin and H. Nilsson, "Assembling surface mounted components on ink-jet printed double sided paper circuit board", *Nanotechnology*, vol. 25, no. 9, p. 094002, 2014.

[19] J. Niittynen, J. Kiilunen, J. Putaala, V. Pekkanen, M. Mäntysalo, H. Jantunen and D. Lupo, "Reliability of ICA attachment of SMDs on inkjet-printed substrates", *Microelectronics Reliability*, vol. 52, no. 11, pp. 2709-2715, 2012.

[20] S. R. Marongelli et al., “Practical production uses of SMT adhesives,” in *Proc. IEEE/CPMT Int. Electron. Manufact. Technol. (IEMT) Symp.*, 1998, pp. 147–155.

[21] B. K. Tehrani, B. S. Cook and M. M. Tentzeris, "Inkjet-printed 3D interconnects for millimeter-wave system-on-package solutions," *2016 IEEE MTT-S International Microwave Symposium (IMS),* San Francisco, CA, 2016, pp. 1-4.

[22] R. A. Lake and R. A. Coutu, "Using Cross-Linked SU-8 to Flip-Chip Bond, Assemble, and Package MEMS Devices," in *IEEE Transactions on Components, Packaging and Manufacturing Technology*, vol. 5, no. 3, pp. 301-306, March 2015.

[23] Deffenbaugh, Paul I., Raymond C. Rumpf, and Kenneth H. Church. "Broadband Microwave Frequency Characterization of 3-D Printed Materials". *IEEE Transactions on Components, Packaging and Manufacturing Technology* 3.12 (2013): 2147-2155. Web.

[24] M. Lis, M. Plaut, A. Zai, D. Cipolle, J. Russo, J. Lewis and T. Fedynyshyn, "Polymer Dielectrics for 3D-Printed RF Devices in the Ka Band," *Advanced Materials Technologies*, vol. 1, no. 2, pp. 160027, May, 2016